JOURNAL OF PROPULSION AND POWER
Vol. 18, No. 4, July–August 2002

Orbital Performance Measurements of Air Force Electric Propulsion Space Experiment Ammonia Arcjet

J. M. Fife* and D. R. Bromaghim†
Air Force Research Laboratory, Edwards Air Force Base, California 93524
D. A. Chart‡
General Dynamics, Inc., Kirtland Air Force Base, New Mexico 87117
W. A. Hoskins§ and C. E. Vaughan¶
General Dynamics, Inc., Redmond, Washington 98052
and
L. K. Johnson**
The Aerospace Corporation, El Segundo, California 90245

During the Electric Propulsion Space Experiment mission, eight firings of the 26-kW ammonia arcjet were performed. Data from onboard systems, including an accelerometer and global positioning system unit, are used to determine thruster performance. In addition, ground-based tracking is used to determine velocity change during these firings. The mean values of thrust, specific impulse, and thrust efficiency are estimated to be 1.93 ± 0.06 N, 786.2 ± 43.0 s, and 0.267 ± 0.021, respectively. This measured performance is lower than expected based on ground test. The most likely cause of this discrepancy is error in onboard measurement of discharge power due to a 6% drift in the power processing unit current shunt. At the corrected power, performance falls within the expected envelope.

Nomenclature

A'	=	venturi calibration parameter
a	=	spacecraft acceleration
BIAS′	=	accelerometer output bias
F	=	thrust
g	=	gravitational acceleration
I_{sp}	=	specific impulse
$\dot{m}$	=	propellant flow rate
P	=	arcjet input power
p	=	absolute pressure
SF′	=	temperature-dependent accelerometer scaling factor
SMA	=	semimajor axis
T	=	temperature
$\mathcal{T}P$	=	orbital period
u	=	uncertainty
V_a	=	accelerometer output voltage
$V_{a,0}$	=	accelerometer instrumentation bias
ΔV	=	spacecraft velocity change
η	=	thrust efficiency

Received 22 January 2001; revision received 2 January 2002; accepted for publication 27 January 2002.

*Research Scientist, Spacecraft Propulsion Branch, 1 Ara Road. Member AIAA.
†Program Manager, Spacecraft Propulsion Branch, 1 Ara Road. Member AIAA.
‡Space and Missile Systems Center, Detachment 12, Space Vehicle Operations, 3548
§Senior Principal Development Engineer, Systems and Technology Development, Space Propulsion Systems, 7025 137th Avenue Northeast.
¶Director, Space Systems Engineering, Space Propulsion Systems, 17507 Northeast 156th Street, Woodinville, WA 98072.
**Electric Propulsion Space Experiment Chief Scientist, currently research Scientist, Thermal and Propulsion Engineering, Jet Propulsion Laboratory, Mail Stop 125-109, 4800 Oak Grove Drive, California Institute of Technology, Pasadena, CA 91109; lee.k.johnson@jpl.nasa.gov. Member AIAA.

Introduction

THE Electric Propulsion Space Experiment (ESEX) is a 30-kW ammonia arcjet experiment sponsored by the U.S. Air Force Research Laboratory. The experiment objectives are to demonstrate the feasibility and compatibility of a high-power arcjet system, as well as to measure and record flight data for subsequent comparison to ground results.[1–3]

ESEX is one of nine experiments launched on 23 February 1999 on the U.S. Air Force Advanced Research and Global Observation Satellite (ARGOS). ARGOS was launched on a Delta II into a 460 nl mile, 98.7-deg inclination orbit[4,5] and operated from the Research and Development, Test, and Evaluation Support Complex at the U.S. Air Force Space and Missile Test and Evaluation Directorate at Kirtland Air Force Base, New Mexico.

ESEX flight system was designed and built as a self-contained experiment, thermally isolated from ARGOS to minimize any effects due to the arcjet firings. ESEX includes a propellant feed system (PFS)[6]; a power subsystem,[7] including the power conditioning unit (PCU)[8] and silver–zinc battery; the commanding and telemetry modules; an onboard diagnostics suite,[1] and the arcjet assembly.[8] The flight diagnostic suite includes four thermoelectrically cooled quartz crystal microbalance sensors, four radiometers, near- and far-field electromagnetic interference antennas, a section of eight gallium–arsenide (Ga–As) solar array cells, a video camera, and an accelerometer.

This paper concentrates on analysis of the performance data and summarizes overall performance findings. Details about performance-related flight instrumentation and specific data reduction processes may be found in previous publications.[9] Information about other ESEX flight instruments (not performance related) may be found in Refs. 10–13.

Description of Experiment

One of the primary objectives of the ESEX flight experiment is to determine the on-orbit performance of the arcjet in terms of specific impulse, thrust, and efficiency. A variety of instruments and techniques were used to collect and analyze data to obtain these results. Performance-measuring instrumentation built into the ESEX flight unit includes a servoaccelerometer assembly (SAA), pressure and temperature sensors in the PFS to determine flow rate, and

Table 1 Arcjet firing summary

Firing	Date, 1999	Time (Zulu), hr	Duration h/min	Flow rate mg/s	Remarks
1	15 March	2155:56	2/20	240	Indicated arcjet power was lower than expected
2	19 March	2232:24	5/02	250	——
3	21 March	1224:42	5/34	250	——
4	23 March	2127:59	8/02	250	Shut-off due to low battery voltage
5	26 March	1245:29	6/05	250	Shut-off due to low battery voltage
6	31 March	1305:36	4/31	250	Shut-off due to low battery voltage
7a	2 April	2209:03	0/55	250	Shut-off due to low battery voltage, low power
7b	2 April	2210:08	0/37	250	Shut-off due to low battery voltage, low power
8	21 April	1222:13	0/43	250	Shut-off due to low battery voltage, low power

electronics in the PCU to determine the arcjet discharge current and voltage. Onboard global positioning system (GPS) data and ground-based tracking data from the Air Force Satellite Control Network (AFSCN) were also used to make an independent measurement of ΔV due to arcjet firings.

Table 1 is a summary of the arcjet firing events. In firings 1–6, the peak PCU-regulated discharge power is estimated at 27.8 kW ±0.18%. In firings 4–8, battery problems forced early shutoff of the arcjet PCU. Because of an onboard battery failure, firings 7 and 8 never reached full power. Indicated arcjet power was lower than expected during firing 1. Subsequently, flow rate was increased from 240 to 250 mg/s for firings 2–8. Additional information about ESEX operation (including firing history) may be found in Ref. 10.

Flight Measurements

To calculate arcjet performance, a variety of measurements were taken onboard ESEX during arcjet operation. Thrust, specific impulse, and efficiency could then be calculated with

$$F = ma \tag{1}$$

$$I_{sp} = F/\dot{m}g \tag{2}$$

$$\eta = F^2/2\dot{m}P \tag{3}$$

In addition, thrust and resulting spacecraft acceleration could be verified with ground-based tracking data and with an onboard GPS unit.

Accelerometer

The onboard SAA measures spacecraft acceleration. The SAA housing is 2.2 × 2.8 × 5.5 in. in size and contains the accelerometer and associated amplifier, bias, and filter electronics. The analog signal from the SAA is digitized and recorded by the ESEX Command/Control Unit (CCU) at 10 Hz. Then 10 readings of digital data are collected and transferred from the ESEX CCU to ARGOS at 1 Hz and recorded for later downlink to a ground station. Figure 1 shows the signal/data path.

The accelerometer is an Allied Signal QA-3000-010, the performance properties of which are given in Table 2. The QA-3000-001 uses a pendulum proof mass made of fused quartz to sense acceleration. Displacement is measured with a capacitive sensor. A closed-loop feedback circuit balances the acceleration force on the proof mass using electromagnetic coils. The current driven through the electromagnet coils thus provides a proportional measure of acceleration. This current is passed through a 20-kΩ shunt in the SAA electronics. The shunt voltage is then filtered, amplified, and biased by other electronics in the SAA. The resulting signal output from the SAA (0–10 V) is digitized in the CCU's 12-bit A/D converter.

Calibrated mean acceleration is calculated by taking the 12-bit SAA output voltage V_a and subtracting an instrumentation bias $V_{a,0}$. The result is divided by a scaling factor (SF) that represents the combined effect of the accelerometer response, input resistance, and instrumentation gain. Finally, a correction is applied for temperature dependency and long-term drift [BIAS′(T)]. To summarize,

Table 2 QA-3000-001 accelerometer specifications

Property	Value
Measurement range	±25 g
Resolution	1 μg
Unbiased output noise at DC to 10 Hz	10 μg

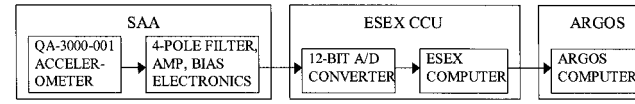

Fig. 1 Accelerometer signal/data path.

$$a = \frac{V_a - V_{a,0}}{\mathrm{SF}'(T)} - \mathrm{BIAS}'(T) \tag{4}$$

Equation (4) gives the instantaneous acceleration. To calculate the mean acceleration $\bar{a}$ for a given firing, V_a and SF′(T) are taken to be the 30-s averages immediately before arcjet shutoff. BIAS′(T) is the accelerometer signal bias, measured by averaging the accelerometer signal for 30-s before arcjet startup (zero acceleration).

The uncertainty in the mean acceleration, $u(\bar{a})$ is derived using standard methods for independent measurands.[14] The uncertainty in V_a and $V_{a,0}$ is dominated by A/D converter discretization error. It is assumed to be 1 bit of resolution, which corresponds to 3.05% of nominal. Combining all measurement uncertainties,[9] we have $u(\bar{a}) = 3.44$ μg, or 4.44% of nominal.

GPS

It was the intent of the ESEX team to use GPS receiver data from ARGOS to make an assessment of the ESEX acceleration profile independent of the SAA. Because of problems with the GPS unit and its interface with the ARGOS navigation system, however, data are only available for firing 1. The analysis of the existing GPS data is complicated because the receiver frequently switched between GPS satellites and intermittently went in and out of lock. For this reason, an instantaneous, GPS-derived acceleration profile cannot be determined. However, after considerable postprocessing, an estimate of ΔV was determined for firing 1 of 0.110 ± 0.003 m/s.

Ground-Based Tracking

Ground-based tracking from AFSCN is also used as an independent measurement of total velocity change during the firing. Tracking data are not precise enough to determine the instantaneous acceleration profile during a firing. However, the total change in semimajor axis from a firing can be determined. From this, ΔV is calculated.

Tracking data are used to determine orbit just before the propulsive event, and again after the event, once sufficient track data has been collected. Track data includes pseudorandom noise ranging, range rate, and antenna pointing angles from the AFSCN antenna network. An orbit solution is typically based on eight tracking passes over 12–18 h, depending on available network assets. The

computational orbit determination scheme operates by successively correcting the orbit parameters to minimize the residual of position error in a least-squares sense using the aforementioned measurements as the observables.[15]

Once the orbit has been determined before and after the propulsive event, each solution is computationally propagated for five-day periods. Brouwer mean (BM) elements are computed for each period. Then, the difference in semimajor axis (ΔSMA) is computed by taking the time average of the difference of the BM SMAs. This process serves to minimize the effects of local perturbations to the orbit. The thrust direction was retrograde, and so, using the circular orbit approximation,

$$\Delta V = \pi \Delta \mathrm{SMA} / \overline{TP} \tag{5}$$

The errors in SMA are computed from the in-track position differences between adjacent orbit solutions. For the investigated period, the statistical bound on the error in SMA is approximately ± 2.5 m. This high SMA precision is due to the use of a trajectory model in which orbit parameters are supported by multiple observables, not just spacecraft position. The uncertainty in ΔV is then determined as,

$$u(\Delta V) = \pi u(\mathrm{SMA}) / \overline{TP} \tag{6}$$

Mass History

The spacecraft mass was measured before launch to be 2491 ± 5 kg, but this decreased throughout the ESEX mission as a result of the following: 1) material outgassing, 2) carbon dioxide gas release from the cold gas attitude control thrusters, 3) xenon and carbon dioxide gas released as part of the critical ionization velocity experiment [4] and 4) arcjet firings. The total mass released by these events through firing 8 is estimated to be 9 ± 2 kg. The spacecraft mass during each firing ranges between 2488 kg (firing 1) and 2482 kg (firing 8) with uncertainty of 6 kg.

Propellant Flow Rate

The PFS on ESEX consists of a sonic venturi with upstream temperature and pressure sensors. Flow rate is calculated by the ESEX CCU at 1 Hz and transferred to ARGOS for downlink. The formula is from fluid mechanics:

$$\dot{m} = \left(p / \sqrt{T}\right) A' \tag{7}$$

The calibration parameter A' accounts for orifice area, flow expansion, etc.

The sonic venturi calibration parameter and the pressure transducer rated accuracy dominate the uncertainty analysis. A root sum of squares combination of these errors gives approximately 4.5% uncertainty in the measurement of $\dot{m}$.

PCU

The PCU provides current-regulated electric power to the arcjet. Both the current and voltage are telemetered from the PCU as 0–5 V signals. They are digitized at 1 Hz by a 12-bit A/D converter in the ESEX CCU and transferred to ARGOS for downlink.

The current and voltage telemetry from the PCU were calibrated during acceptance testing. Uncertainty in power (using the product of voltage and current from telemetry) is determined in this analysis from the statistical variation of error from several independent acceptance tests to be 601 W.

Analysis and Discussion

The calibrated acceleration for a representative firing (firing 5) is given in Fig. 2. Features in the acceleration history correspond to operational phases of the arcjet firing. A valve opens between the pressurized plenum tank and the thruster, 4 minutes before initiation of the arcjet discharge, and propellant flow begins.[10] In this phase, the arcjet is operating as a cold-gas thruster, producing a 20-μg acceleration, which ramps down to 8 μg as excess plenum pressure bleeds off. Next, the arcjet discharge initiates with a programmed

Table 3 Total velocity change ΔV (m/s)

Firing	Acceleration	Ground tracking	GPS
1	0.1089 ± 0.0207	0.11101 ± 0.00129	0.110 ± 0.003
2	0.2590 ± 0.0244	0.26023 ± 0.00129	N/A
3	0.2850 ± 0.0244	0.27304 ± 0.00129	N/A
4	0.4010 ± 0.0326	0.40348 ± 0.00129	N/A
5	0.3203 ± 0.0303	0.32809 ± 0.00129	N/A
6	0.2275 ± 0.0216	0.22699 ± 0.00129	N/A
7	0.0626 ± 0.0177	0.06563 ± 0.00129	N/A
8	0.0248 ± 0.0137	0.02924 ± 0.00129	N/A

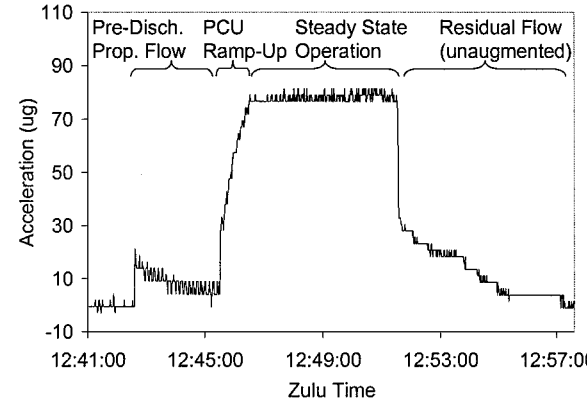

Fig. 2 Calibrated acceleration during firing 5.

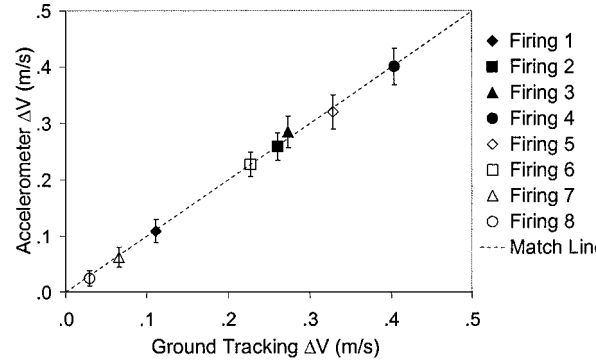

Fig. 3 Comparison between ΔV from accelerometer measurement and ground tracking.

startup sequence. This is seen as a ramp in acceleration from 8 to 76 μg. After the ramp, the PCU switches to constant power mode at approximately 26 kW. The exponential dropoff of acceleration occurs after the arcjet discharge is shut off. Nominal flow continues for 5 to 6 min after shutoff as the plenum tank bleeds down. This generates additional thrust, which diminishes as the arcjet cools.

Total velocity change ΔV is obtained by integration of the instantaneous acceleration curve. The trapezoidal rule is used, and the uncertainty is computed based strictly on systematic sources assuming the random components cancel. Those numbers are shown in Table 3 in comparison to results from ground tracking and GPS.

Figure 3 shows a graphical comparison of ΔV from the accelerometer data with ΔV from ground tracking. The line represents a perfect match. The slope of a linear least-squares fit is 1.0083, indicating only 0.83% SF error, with an rms relative residual of 3.01%. Thus, the accelerometer data correlate to within 3.1% of independent ground tracking data for all eight firings and with GPS data for firing 1. Thus, there is a high probability that the accelerometer measurements are more accurate than the instrumentation uncertainty analysis predicts. The uncertainty in the measurement of acceleration is, therefore, taken to be 3.1% for the mean steady-state performance analysis to follow.

Average steady-state acceleration is determined from the individual averages of the accelerometer voltage, SF, and bias over the

Table 4 Accelerometer-based performance summary

Firing	Mean acceleration $\bar{a}$, μg	Mean thrust $\bar{F}$, N	Mean specific impulse $\overline{I_{sp}}$, s	Mean efficiency $\bar{\eta}$
1	76.07 ± 2.36	1.856 ± 0.058	789.3 ± 43.2	0.259 ± 0.021
2	78.98 ± 2.45	1.925 ± 0.060	785.7 ± 43.0	0.267 ± 0.021
3	80.97 ± 2.51	1.974 ± 0.061	806.0 ± 44.1	0.281 ± 0.022
4	78.34 ± 2.43	1.909 ± 0.059	779.3 ± 42.6	0.262 ± 0.021
5	77.64 ± 2.40	1.887 ± 0.059	770.7 ± 42.2	0.257 ± 0.020
6	79.42 ± 2.46	1.933 ± 0.060	789.5 ± 43.2	0.270 ± 0.022

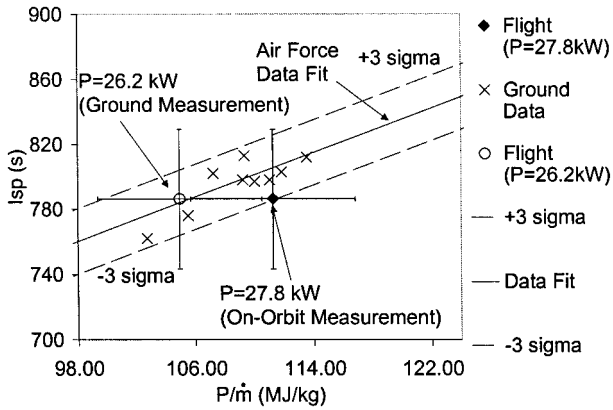

Fig. 4 Summary of specific impulse estimates.

last 30-s of each firing. Likewise, performance parameters are determined from the individual 30-s averages of the acceleration, flow rate, and discharge power. Table 4 is a summary of the steady-state results.

Final performance figures can be determined as the mean of the five 30-s means from firings 2–6. This gives, for the 250 mg/s flow rate,

$$\bar{\bar{F}} = 1.93 \pm 0.06 \text{ N}, \qquad \overline{\overline{I_{sp}}} = 786.2 \pm 43.0 \text{ s}$$

$$\bar{\bar{\eta}} = 0.267 \pm 0.021$$

The uncertainties are computed as the root mean square (RMS) of the uncertainties of the individual firings. Therefore, final mean accelerometer-based measurements of F, I_{sp}, and η are believed accurate to 3.1, 5.4, and 7.9%, respectively.

The original design specification for the arcjet requires F, I_{sp}, and η to be 1.96 N, 800 s, and 0.307, respectively. These measurements indicate that the F and I_{sp} specifications were met during on-orbit operation within the uncertainty of the instrumentation. However, η, fell below the specification.

Figure 4 shows the mean specific impulse in comparison with ground data. The vertical error bars represent uncertainty in I_{sp}, taking into account the uncertainty in power and flow rate. The horizontal error bars represent the combined standard uncertainty for $P/\dot{m}$, with $u(P) = 2.2\%$ and $u(\dot{m}) = 4.5\%$. The diagonal lines represent a regression fit of previous Air Force NH_3 arcjet data and 3σ bounds on that fit.[16] It is within this 3σ envelope that flight measurements are expected to fall. It is clear from Fig. 4 that the mean on-orbit I_{sp} is somewhat low for the corresponding $P/\dot{m}$.

The lower-than-expected I_{sp} may be due to erroneous power measurements. During acceptance tests, power was measured externally at 26.2 ± 1.5 kW (Ref. 17). However, during on-orbit thruster firings, the voltage and current telemetry consistently indicated a power reading of 27.8 ± 0.05 kW, 6% higher. An examination of the data, both on-orbit and during acceptance testing in 1994, indicates that the power reading is higher than actual, due, most likely, to a drift in the telemetry current. Arcjet temperatures and on-orbit performance data corroborate this conclusion. Also, the PCU is designed to be resistant to changes in power. Furthermore, during acceptance tests, while the independently measured power remained constant, a drift was observed in the original flight shunt (which was subsequently rejected and replaced). Although there is no way to positively identify the source of the discrepancy, these indications suggest that the current telemetry is erroneous (reading 6% too high). If the PCU is treated as a constant-power device, with actual power levels corresponding to those during acceptance tests (26.2 kW ± 1.5%), the thrust efficiency increases 6% to 0.283 ± 0.029, which meets specification within the uncertainty. Furthermore, $P/\dot{m}$ for the 250 mg/s firings becomes 105 MJ/kg, which centers the mean I_{sp} in the expected range. The point labeled $P = 26.2$ kW in Fig. 4 represents this case. However, because irrefutable evidence of current shunt drift is not available, the higher performance cannot be reported with complete confidence.

Summary

Based on accelerometer data alone, mean arcjet thrust, specific impulse, and thrust efficiency are 1.93 ± 0.06 N, 787.0 ± 43.0 s, and 0.268 ± 0.021, respectively. These values, except for efficiency, meet design specification within the measured uncertainties. A likely explanation for the discrepancy in measured mean efficiency is drift in the PCU current telemetry. Assuming a 6% drift in PPU current telemetry, efficiency increases to 0.283 ± 0.021, meeting specification.

The dominant contributors to uncertainty in accelerometer-based performance measurement are encoding error of the A/D converter and uncertainty in flow rate. Although these factors lead to large uncertainty in measured acceleration (4.44%), measurements of ΔV from GPS and ground tracking independently support the accelerometer data to a higher accuracy (3.1%).

To use the results presented in design of spacecraft with operational ammonia arcjets, some points must be considered. First, these performance results are for steady-state operation. The additional propellant released before and after firing and the rampup to full power must be taken into account in a more complete analysis. Also, uncertainty in measured performance presented here is high. Therefore, if these numbers are used for design, propellant/power margin should be included in accordance with the uncertainty.

Acknowledgments

The authors would like to thank the following people for their support of the Electric Propulsion Space Experiment mission: the TRW Arcjet Advanced Technology Demonstration Program team, The Boeing Company, the Delta II launch crew at Vandenberg Air Force Base Space and Missile Command, Test Evaluation Division, and Space and Missile Command, Space Test Programm Office. In addition, the authors would like to thank Alan Sutton and Jason LeDuc for assistance during flight operations and for their contributions to this performance analysis.

References

[1]Kriebel, M. M., and Stevens, N. J., "30-kW Class Arcjet Advanced Technology Transition Demonstration (ATTD) Flight Experiment Diagnostic Package," AIAA Paper 92-3561, July 1992.

[2]Sutton, A. M., Bromaghim, D. R., and Johnson, L. K., "Electric Propulsion Space Experiment (ESEX) Flight Qualification and Operations," AIAA Paper 95-2503, July 1995; also JANNAF Paper, Dec. 1995.

[3]LeDuc, J. R., McFall, K. M., Tilley, D. L., Sutton, A. M., Pobst, J. A., Bromaghim, D. R., and Johnson, L. K., "Performance, Contamination, Electromagnetic, and Optical Flight Measurement Development for the Electric Propulsion Space Experiment," AIAA Paper 96-2727, July 1996.

[4]Turner, B. J., and Agardy, F. J., "The Advanced Research and Global Observation Satellite (ARGOS) Program," AIAA Paper 94-4580, Sept. 1994.

[5]Agardy, F. J., and Cleave, R. R., "A Strategy for Maximizing the Scientific Return Using a Multi-phased Mission Design for ARGOS," American Astronautical Society, AAS Paper 93-594, Aug. 1993.

[6]Vaughan, C. E., and Morris, J. P., "Propellant Feed Subsystem for a 26-kW Flight Arcjet Propulsion System," AIAA Paper 93-2400, June 1993.

[7]Biess, J. J., and Sutton A. M., "Integration and Verification of a 30-kW Arcjet Spacecraft System," AIAA Paper 94-3143, June 1994.

[8]Vaughan, C. E., Cassady, R. J., and Fisher, J. R., "Design, Fabrication, and Test of a 26 kW Arcjet and Power Conditioning Unit," International Electric Propulsion Conf., IEPC Paper 93-048, Sept. 1993.

[9]Fife, J. M., LeDuc, J. R., Sutton, A. M., Bromaghim, D. R., Chart, D. A., Hoskins, W. A., Vaughan, C. E., and Johnson, L. K., "Preliminary

Orbital Performance Analysis of the Air Force Electric Propulsion Space Experiment (ESEX) Ammonia Arcjet," AIAA Paper 99-2707, June 1999.

[10]Bromaghim, D. R., LeDuc, J. R., Salasovich, R. M., Spanjers, G. G., Fife, J. M., Dulligan, M. J., Schilling, J. H., White, D. C., and Johnson, L. K., "Review of the Electric Propulsion Space Experiment Program," *Journal of Propulsion and Power*, Vol. 18, No. 4, 2002, pp. 723–730.

[11]Spanjers, G. G., Schilling, J. H., Engelman, S. F., Bromaghim, D. R., and Johnson, L. K., "Mass Deposition Measurements from the 26-Kilowatt Electric Propulsion Space Experiment Flight," *Journal of Propulsion and Power*, Vol. 18, No. 4, 2002, pp. 772–776.

[12]Schilling, J. H., Spanjers, G. G., Bromaghim, D. R., and Johnson, L. K., "Solar Cell Degradation During the 26-Kilowatt Electric Propulsion Space Experiment Flight," *Journal of Propulsion and Power*, Vol. 18, No. 4, 2002, pp. 768–771.

[13]Spanjers, G. G., Schilling, J. H., Bromaghim, D. R., and Johnson, L. K., "Radiometric Analysis from the 26-Kilowatt Electric Propulsion Space Experiment Flight," *Journal of Propulsion and Power*, Vol. 18, No. 4, 2002, pp. 777–780.

[14]*American National Standard for Expressing Uncertainty—U.S. Guide to the Expression of Uncertainty in Measurement*, American National Standard Inst./National Conference on Standard Laboratories, 1800 30th St., Suite 305B, Boulder, Colorado, 80301. Rept. ANSI/NCSL Z540-2-1997, Oct. 1997.

[15]OASYS Mathematical Foundations for OASYS Ver. 3.x, Integral Systems, Lanham, MD, April 1998.

[16]Cassady, R. J., Lichton, P. G., and King, D. Q., "Arcjet Endurance Test Program Final Report," Air Force Research Laboratory, Propulsion Directorate, Scientific and Technical Information Office, 5 Pollux Dr., Edwards AFB, CA 93524. AL-TR-90-069, March 1991.

[17]Cassady, R. J., Hoskins, W. J., and Vaughan, C. E., "Qualification of a 26-kW Arcjet Flight Propulsion System," AIAA Paper 95-2502, July 1995.